Chemical Research in Toxicology

Article

pubs.acs.org/crt

Cadmium-Based Quantum Dot Induced Autophagy Formation for Cell Survival via Oxidative Stress

Yueh-Hsia Luo,[†] Shi-Bei Wu,[‡] Yau-Huei Wei,[§] Yu-Ching Chen,[∥] Ming-Hsien Tsai,[†] Chia-Chi Ho,[†] Shu-Yi Lin,[∥] Chung-Shi Yang,[∥] and Pinpin Lin*[,†]

[†]Division of Environmental Health and Occupational Medicine, National Health Research Institutes, Zhunan, Taiwan, Republic of China

[‡]Department of Biochemistry and Molecular Biology, National Yang-Ming University, Taipei 112, Taiwan, Republic of China

[§]School of Medicine, Mackay Medical College, New Taipei City 252, Taiwan, Republic of China

[∥]Center for Nanomedicine Research, National Health Research Institutes, Zhunan, Taiwan, Republic of China

Supporting Information

ABSTRACT: Quantum dots (QDs) are one of most utilized nanomaterials in nanocrystalline semiconductors. QDs emit near-infrared fluorescence and can be applied as probes for detecting vasculature and imaging in biological systems. Since QDs have potential in clinical application, the toxicity of QDs needs to be carefully evaluated. In our present study, we elucidate the cytotoxic mechanisms of QDs using a mouse renal adenocarcinoma (RAG) cell line. QDs in RAG cells increased intracellular reactive oxygen species (ROS) levels and induced autophagy at 6 h, leading to subsequent apoptosis at 24 h. QDs entered the cells and were located within the endoplasmic reticulum (ER), endosome, and lysosome at 6 h and endosome, lysosome, and mitochondria at 24 h. However, QDs only affected mitochondrial function and did not induce ER stress. *N*-Acetylcysteine, an antioxidant agent, reduced intracellular ROS levels and decreased QD-induced autophagy but enhanced QD-induced cell death. Moreover, 3-methylamphetamine (an autophagy inhibitor) also reduced the cell viability in QD-treated cells. These findings suggest that ROS plays an essential role in the regulation of QD-induced autophagy, which subsequently enhances cell survival. Taken together, these results suggest that oxidative stress-induced autophagy is a defense/survival mechanism against the cytotoxicity of QD.

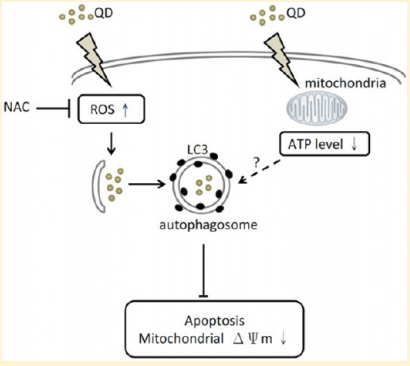

INTRODUCTION

Quantum dots (QDs) are a class of semiconductor nanocrystals with a size typically ranging between 1.5 and 12 nm.[1,2] As a result of their specific excitation frequencies and broad emission spectrum properties, QDs can be used as novel luminescent materials in certain biological assays. A number of authors have suggested that QDs potentially have applications as multimodal contrast agents during drug delivery[3,4] and in bioimaging, including magnetic resonance imaging, positron emission tomography, computed tomography, and infrared (IR) fluorescence imaging.[2,5,6] QDs are commonly used as a fluorescent probe for bioimaging fixed cells and tissues. In biomedical research, an important utilization is labeling transplantation cells with QDs enabling the follow up of cells by noninvasive fluorescence imaging and histological examinations.[7] QDs also can be conjugated with bioactive moieties such as receptor ligands in order to label certain specific cells.[8,9] Since QDs have significant potential in terms of drug targeting and biomedical imaging, the toxicity of QDs needs to be carefully evaluated.

The toxicity of QDs is dependent on their physicochemical properties, such as the size, charge, core composition, and stability of the outer surface layers.[10,11] Several metal complexes have been used for the QD core, including zinc−selenium (ZnSe), cadmium−selenium (CdSe), and cadmium−tellurium (CdTe).[12,13] The outer coating material shields the inner metal core in order to enhance the quantum yield and solubility. Toxic metals can potentially leak out from the QD when the outer coating material degenerates due to oxidation or under low pH.[14,15] It has been reported that the leaking of toxic core metals is able to generate reactive oxygen species (ROS), which cause lipid peroxidation, damage cellular membrane integrity, and cause oxidative damage to DNA and cellular proteins, all of which might finally lead to cell death.[16−18] It is desirable that QDs with appropriate surface modification would make QDs selectively bind with specific target cells such as tumors but not normal cells. QD surface modification technology is still not good enough to prevent nontargeted bonding, so there is always a risk of damaging normal cells.[2] Owing to the complexity of surface chemistry, as well as the lack of long-term studies determining successful clearance of QD, safety still remains a major problem for in vivo application of QD nanotechnology.[1,2,19]

Received: November 14, 2012
Published: April 25, 2013

Several studies have demonstrated that nanoparticles (NPs) activate autophagy via a size-dependent mechanism.[20−24] Autophagy is derived from Greek roots: "auto", meaning "self" and "phagy" meaning "to eat".[25] Autophagy means eating parts of oneself in order to survive and occurs in living organisms ranging from yeast to humans under deleterious environments. It has been suggested that the upregulation of autophagy may be an adaptative response to environmental stress.[26] Autophagy may also play a role in the rapid sequestering and recycling of oxidatively damaged proteins and organelles, which would provide a selective advantage in terms of cell survival.[27,28] Growing evidence has revealed that regulation of autophagy is involved in many human diseases, including cancer, infection and immunity, heart disease, liver disease, aging, myopathies, and neurodegeneration.[29] It is also worth noting that NP induction of autophagy may be a way of self-clearance.[20] In addition, several NPs, such as gold NPs, polyamidoamine dendrimer (PAMAM), and QDs, seem to induce autophagy and increase intracellular oxidative stress.[21,22,24] The ROS production by NPs is responsible for inducing cell death and tissue injury and is required for the induction of autophagy. However, the role of ROS production and autophagy in the cytotoxicity of NPs remains unclear.

Our previous studies have reported the toxicokinetics of QDs in mice.[30] QDs are retained in the body for 16 weeks after exposure with significant redistribution over time to the liver and kidneys.[31,32] Time-dependent accumulation of QDs and ultrastructural changes to the mitochondria have been shown to occur in the kidneys of QD-exposed animals.[33] In the present study, we explore the role of autophagy in QD-induced cytotoxicity using mouse renal adenocarcinoma (RAG) cells. Our results suggest that ROS may have an essential role in the regulation of QD-induced autophagy. Oxidative stress-induced autophagy would seem to be a defense/survival mechanism against the cytotoxicity of QDs.

MATERIALS AND METHODS

Materials. The QD705 NPs used in this study were purchased from Invitrogen, Inc. (Hayward, CA, USA) as carboxyl quantum dots 705. The shape and size of NPs were characterized by TEM and DLS (Supporting Information, Figure 1). QD is a spherical shaped NP with a core size of 10 ± 2 nm. The diameter of the QD in MEM medium is 33 nm. The QDs contain a covered Cd/Se core, which has a shell with an additional semiconductor layer (ZnS) to improve their chemical and optical properties. The polymer coating has $-COO^-$ surface groups available for further modifications such as macromolecule attachment. Each tube of this product contained 250 μL of an 8 μM solution in 50 mM borate buffer (pH 9.0). The Cd ion was collected by using the microdialysis system and quantified by inductively coupled plasma mass spectrometry (ICP-MS). The microdialysis system has a microinjection syringe pump (CMA/400) and a 10 mm long probe (CMA/20), which were purchased from CMA (Carnegie Medicine Association, Solna, Sweden). In brief, 50 mM borate buffer solution was infused into the microdialysis system at a flow rate of 1 μL/min. The samples were collected every hour for 24 h and quantified for Cd concentrations using ICP-MS. The free Cd ion content of the QDs was less than 0.01‰ (gm/g). The QDs contained 43% to 47% (g/g) of Cd. Twenty nanomolar QD and 21.66 μg/mL of $CdCl_2$ contain equivalent amounts of Cd: 20 nM QD × molecular weight (1.5×10^6) × percentage of Cd in QD (44%) = 21.66 μg/mL $CdCl_2$ × (molecular weight of Cd/molecular weight of $CdCl_2$). Bovine serum albumin, MEM medium, penicillin/streptomycin, L-glutamine, nonessential amino acids (NEAA), sodium pyruvate, and MitoTracker mitochondrion-selective probes were purchased from Invitrogen, Inc. (Hayward, CA, USA). Thiazolyl Blue Tetrazolium Blue (MTT), *N*-acetylcysteine (NAC), 3-methylamphetamine (3-MA), 2,7-dichlorofluorescein diacetate (DCF-DA), cadmium chloride ($CdCl_2$), and β-actin antibody were acquired from Sigma, Inc. (St Louis, MO, USA). LC3 antibody was purchased from ABGENT Inc. (San Diego, CA, USA). EEA1 (early endosome antigen 1) and Calnexin antibody were obtained from GeneTex, Inc. (San Antonio, TX, USA).

Cell Culture. In the present study, we used a RAG cell line, which is a mouse renal adenocarcinoma cell line derived from BALB/cd mice. The RAG cells were grown as a monolayer with epithelium-like morphology. The cells were cultured in MEM medium with 2 mM L-glutamine, Earle's balanced salts (EBSS), 1.5g/L sodium bicarbonate, 0.1 mM nonessential amino acids, 1.0 mM sodium pyruvate, and 10% fetal bovine serum (FBS).

MTT Cell Viability Assay. Cytotoxicity was determined by the microtiter MTT assay.[34] MTT is a yellow water-soluble tetrazolium dye that is reduced by living cells to a water-insoluble purple formazan. Appropriate cell numbers were (1×10^4/well) plated in 96-well microtiter plates and then treated for 6 and 24 h with or without 10 nM and 20 nM QDs, diluted directly into the MEM media. At 6 and 24 h, 200 μL of MTT solution (1 mg/mL in MEM medium) was added to the wells. The plates were then incubated at 37 °C for 2 h. Following incubation, the MTT incubation medium was removed and 200 μL of dimethyl sulfoxide (DMSO) added to each well. The plates were shaken at room temperature for 15 min, and the absorbance was read at a wavelength of 535 nm on a microplate spectrophotometer (Molecular Devices, Sunnyvale, CA, USA). The relative viability was expressed as a percentage of the nontreated control. The QD only group was examined to rule out the interference of MTT measurement (data not shown).

Lactate Dehydrogenase (LDH) Activity Assay. The CytoTox96 nonradioactive cytotoxicity assay was used to quantitatively measure LDH activity, a stable cytosolic enzyme that is released by cytoplasmic membrane disruption. Such membrane disruption occurs early in necrosis but only at a late stage of apoptosis.[35] The cells were treated with QDs at indicated concentrations for 6 and 24 h, respectively, and the LDH activity released into the conditioned medium was determined according to the manufacturer's instructions (Promega, Madison, WI, USA). The QD only group was examined to rule out the interference of LDH measurement (data not shown).

Transmission Electron Microscopy (TEM). The cells were fixed with a solution containing 2% glutaraldehyde plus 2% formaldehyde in PBS buffer, pH 7.4, at 4 °C. After fixation, the samples were postfixed in 1% OsO_4 in 0.1 M PB buffer at pH 7.4 for 30 min. Ultrathin sections were then observed under a transmission electron microscope (Hitachi H-7650, Japan) at 100 kV.

Fluorescence Imaging of GFP-LC3. The GFP-LC3 plasmid was kindly provided by Dr. Cheng-Wen Wu (National Yang-Ming University, Taiwan). The backbone of the plasmid was used with a pSIN-EF2-Lin28-Pur plasmid purchased from Addgene Inc. (Cambridge, MA, USA). RAG cells were seeded into in 3.5 cm micro-dish (ibidi GmbH, Martinsried, Germany) and incubated for 24 h at 37 °C in a humidified chamber filled with 5% CO_2. After transfection of RAG cells with PolyJet in vitro DNA transfection reagent (SignaGen Laboratories, Ijamsville, MD, USA) for 5 h according to the manufacturer's suggestion, cells were treated with 10 nM QDs for another 18 h. GFP-LC3 transfected RAG cells were subjected to a confocal fluorescence microscope upon excitation by a 473 nm diode laser and the emission measured at 510 nm (Olympus FLUOVIEW FV10i, Penn, USA).

Propidium Iodide (PI) Staining to Assess DNA Fragmentation by Flow Cytometry. The PI staining assay by flow cytometry was used to evaluate the extent of cell death. Apoptotic cells are characterized by a hypoploid DNA fluorescence pattern.[36] The cells were initially seeded at 5×10^5 cells in six-well dishes and then treated with QDs for 24 h. Following treatment, all cells were collected. Cells were then centrifuged, washed once in phosphate-buffered saline (PBS, pH 7.2), and resuspended in 100 μL of PBS. Cells were then added dropwise to 1 mL of ice-cold 70% EtOH with vortexing and stored at −20 °C for at least 30 min. The fixed cells were collected by centrifugation, washed once in PBS, and incubated in 1 mL of PI staining buffer (4 μg/mL PI, 100 μg/mL RNaseA, and 1% Triton X-

dx.doi.org/10.1021/tx300455k | Chem. Res. Toxicol. 2013, 26, 662−673

100 in PBS) for 30 min at room temperature. Each sample was then analyzed using a FACSCalibur flow cytometer upon excitation by a 488 nm argon laser, the emission measured at 564−606 nm (BD Inc., San Jose, CA, USA), and the sub-G1 peak quantified using WinMDI software. The QD only group was examined to rule out the interference of PI staining (data not shown).

Terminal Deoxynucleotidyl Transferase-Mediated dUTP Nick-End Labeling (TUNEL) Assay Staining. For the TUNEL assay, the RAG cells were stained using the In Situ Cell Death Detection kit (Roche Molecular Biochemicals, Indianapolis, IN), according to the manufacturer's instructions. The TUNEL positive cells were detected by confocal microscopy upon excitation at 473 nm and the emission measured at 510 nm.

Measurement of Intracellular ROS. ROS generation was determined using 2,7-dichlorofluorescein diacetate (DCF-DA). Cells (3×10^5/sample) were plated in 96-well black microtiter plates and then treated for 6 and 24 h with or without 10 nM and 20 nM QD and $CdCl_2$, diluted directly into the MEM media. At 6 and 24 h, condition medium was removed, and then, the cells were incubated with 5 μM DCF-DA at 37 °C for 30 min and then immediately measured using a microplate reader with excitation at 485 nm and emission at 520 nm. The QD only group was examined to rule out the interference of DCF measurement (data not shown). Treatment with 10 μM H_2O_2 for 2 h was used as a positive control group. After DCF measurement, the cell viability was detected by using a WST-8 cell proliferation kit (Dojindo Molecular Technologies, Inc.). WST-8 can be reduced by cellular dehydrogenases to an orange formazan product that is soluble in culture medium. The amount of formazan produced is directly proportional to the number of living cells. The ROS production was normalized with cell viability.

Quantitative Real-Time Reverse Transcription−Polymerase Chain Reaction (RT−PCR) Assays. The cells were treated with QDs for 6 and 24 h, and then RNA was extracted using a RNAzol RT kit (Life Technologies, Rockville, MD, USA). The purified RNA was stored at −80 °C, and cDNA was synthesized with total RNA (3 μg). Quantitative PCR was used to measure activating transcription factor 4 (ATF4) and transcription factor C/EBP homologous protein (CHOP), and the assays were performed using the Assay-on-Demand Gene Expression Assay Mix (Applied Biosystems, Foster City, CA, USA). The assay ID of ATF-4 was Mm00515324_m1, of CHOP was Mm00492097_m1, and of glyceraldehyde-3-phosphate dehydrogenase (GAPDH) was Mm99999915_g1. Quantitative PCR to measure ATF4, CHOP, and GAPDH was performed using TaqMan Universal PCR Master Mix (Applied Biosystems, Foster City, CA, USA). The reaction mixture was prepared by mixing aliquots of cDNA, 0.5 μL of Assay-on-Demand Gene Expression Assay Mix, and 5 μL of TaqMan Universal PCR Master Mix (Applied Biosystems, Foster City, CA, USA) in a final volume of 10 μL. The reaction mixture was analyzed on an ABI PRISM 7900 Sequence Detector System (Applied Biosystems, Foster City, CA, USA) with the following PCR program: 95 °C for 10 min, followed by 40 cycles of 60 °C for 1 min, and 95 °C for 15 s. Quantitative values were obtained from the threshold cycle (Ct) number. The relative mRNA levels of the target genes were derived using the eq $2^{-\Delta Ct}$, where $\Delta Ct = Ct_{\text{target gene}} - Ct_{\text{GAPDH}}$. Data are presented as the fold relative to the control value.[32]

Mitochondrial ATP Measurement. Mitochondrial ATP generation was determined by the Mitochondrial ToxGlo assay (Promega, Madison, WI, USA). RAG cells were cultured in glucose-containing medium, then the culture medium was removed and the cells washed and incubated with galactose-containing medium to rule out an inhibition of glycolysis during QD treatment. RAG cells (10^4/well) were treated with QDs for 2 h, 6 h, and 24 h, and then were incubated with 5-fold cytotoxicity reagent at 37 °C for 30 min according to the manufacturer's instructions. The cells were assayed using a microplate reader with excitation at 485 nm and emission at 520−530 nm. After measurement of the fluorescence, the cells were then incubated with ATP detection reagent. The luminescence of the cells was then measured after 5 min. The percentage cell cytotoxicity and cellular level of ATP were expressed as a percentage of the nontreated control.

Mitochondrial Membrane Potential ($\Delta\Psi$m). To assess the changes in mitochondrial $\Delta\Psi$, the RAG cells were stained with 3,3′-dihexyloxacarbocyanine iodide (DiOC6 (3)), a membrane potential-sensitive dye, and analyzed by flow cytometry upon excitation by a 488 nm argon laser and the emission measured at 515−545 nm.[37] In brief, RAG cells were treated with QDs for 24 h, then harvested and washed with PBS (pH 7.2) three times. The cells were loaded with 4 μM DiOC6 (3) at room temperature for 15 min before FACS analysis. Carbonyl cyanide 3-chlorophenylhydrazone (CCCP, 5 mM) was used at room temperature for 10 min as a control for mitochondrial membrane depolarization. $\Delta\Psi$m was measured prior to and immediately after the addition of CCCP. The mean fluorescence of the untreated cells was set at 100%, and the $\Delta\Psi$m of QD-treated cells is given as the percentage fluorescence of untreated cells.

Immunofluorescence Staining. RAG cells were seeded in 3.5 cm micro-dish (ibidi GmbH, Martinsried, Germany) or on coverslips coated with 0.1% collagen in HBSS buffer in six-well dishes and then treated with QDs for 24 h. Next, the cells were fixed with 4% paraformadehyde/0.1% Triton X-100 in PBS (pH 7.2) at room temperature for 20 min and then washed with PBS three times. The cells were blocked with 5% skim milk at room temperature for 1 h. Adequately diluted primary antibodies were then applied to the cells and the mixture incubated at 4 °C overnight. The cells were then washed in PBS and incubated with fluorescein isothiocyanate (FITC)-labeled secondary antibodies at room temperature for 30 min. LC3 was detected using rabbit antihuman LC3, which cross-reacts with mouse LC3, and then with FITC-conjugated goat antirabbit IgG antibody (Calbiochem, Millipore Inc., MA, USA). For the intracellular distribution of the QD, calnexin was detected using rabbit antihuman calnexin, which cross-reacts with mouse calnexin, and then FITC-conjugated goat antirabbit IgG was used as the secondary antibody. EEA1 was detected using rabbit antihuman EEA1, which cross-reacts with mouse EEA1, and then FITC-conjugated goat antirabbit IgG was used as the secondary antibody. MitoTracker (Invitrogen, Molecular Probe, Inc. OR, USA) is a cell-permanent probe that contains a mildly thiol-reactive chloromethyl moiety for labeling mitochondria. LysoTracker (Invitrogen, Molecular Probe, Inc. OR, USA) is a fluorescent acidotropic probe for labeling and tracking acidic organelles in live cells and can be used to investigate intracellular lysosomes. The green Mitotracker, Lysotracker, and FITC-conjugated goat antirabbit IgG were detected by confocal microscopy upon excitation by a 473 nm diode laser and the emission measured at 510 nm. The intracellular distributions of the QDs were detected by confocal microscopy upon excitation by a 559 nm diode laser and the emission measured at 592 nm.

Western Blot Analysis. The cells were harvested in harvest buffer (500 mM HEPES, 200 mM sodium molybdate, 25 mM EGTA, 500 mM magnesium chloride, 50% glycerol, 50% NP-40, 100 mM PMSF, 1 mg/mL leupeptin, 2 mg/mL aprotinin, TLCK, TPCK, and 2 mg/mL pepstatin A) together with the phosphatase inhibitor mixture and protease inhibitor mixture (Roche Applied Science, Mannheim, Germany). The lysed cells were further disrupted with ultrasound to completely disassociate the cellular components. After centrifugation at 12,000 rpm at 4 °C for 20 min, the supernatants were collected. Each supernatant was added to an equal volume of 2-fold sample buffer. The protein concentration was determined by the BCA assay (Pierce Biotechology, IL, USA). Equal amounts of protein were resolved by SDS−PAGE and transferred onto a polyscreen PVDF transfer membrane (Perkin-Elmer Life science, Inc. MA, USA). After blocking the membrane with 5% skim milk, it was probed with the designated first and second antibodies, developed using the chemiluminescent HRP substrate method (Millipore) and visualized by exposure to light film (Super RX Fuji medical X-ray film, Fujifilm Europe GmbH, Dusseldorf, Germany) in order to reveal each specific protein.

Statistical Analysis. The statistical analysis was carried out on Prism 4.0 software (GraphPad Software, San Diego, CA). Significant differences between treatment groups were determined by an unpaired t test. Differences were considered statistically significant at $^*p < 0.05$, $^{**}p < 0.01$, and $^{***}p < 0.001$.

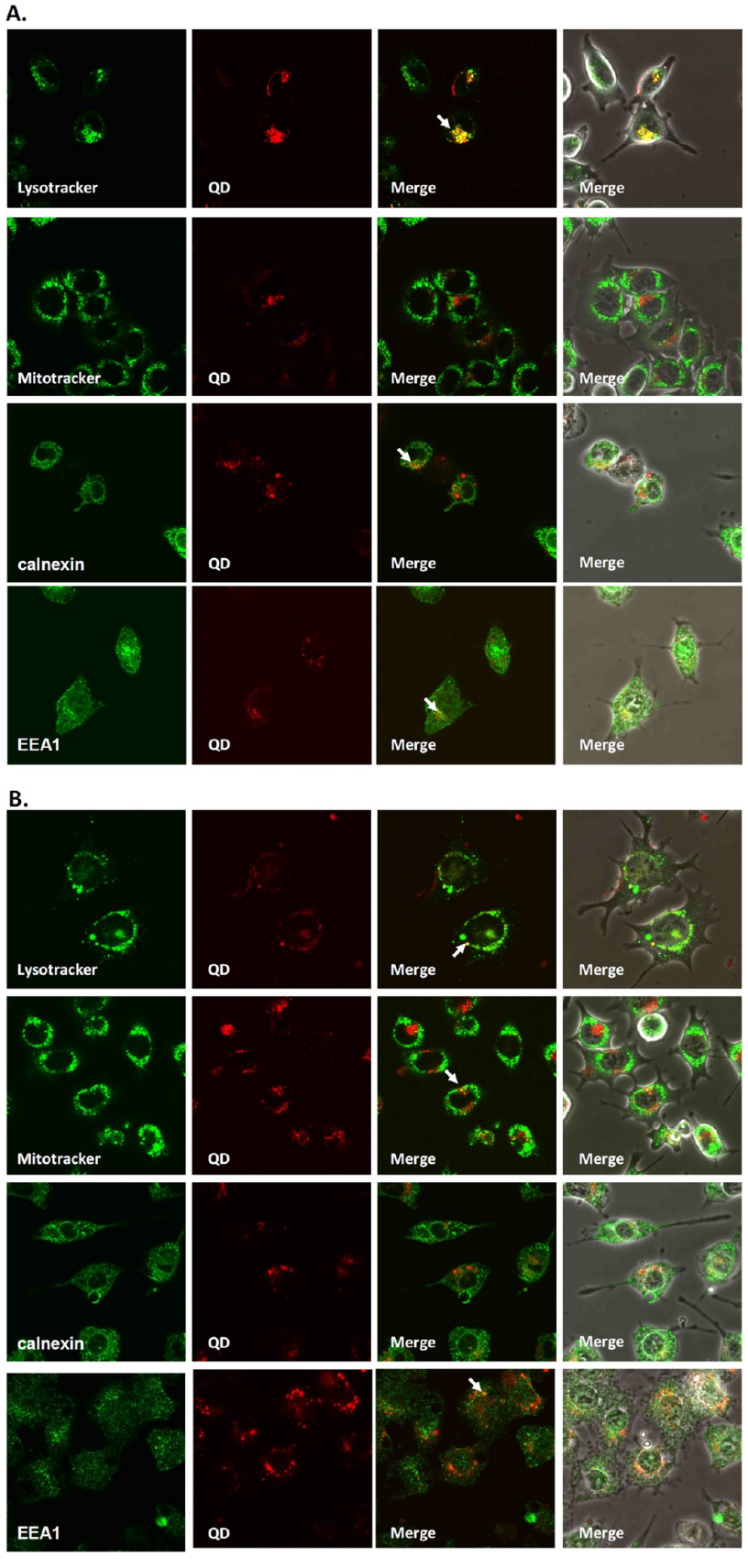

Figure 1. continued

dx.doi.org/10.1021/tx300455k | *Chem. Res. Toxicol.* 2013, 26, 662−673

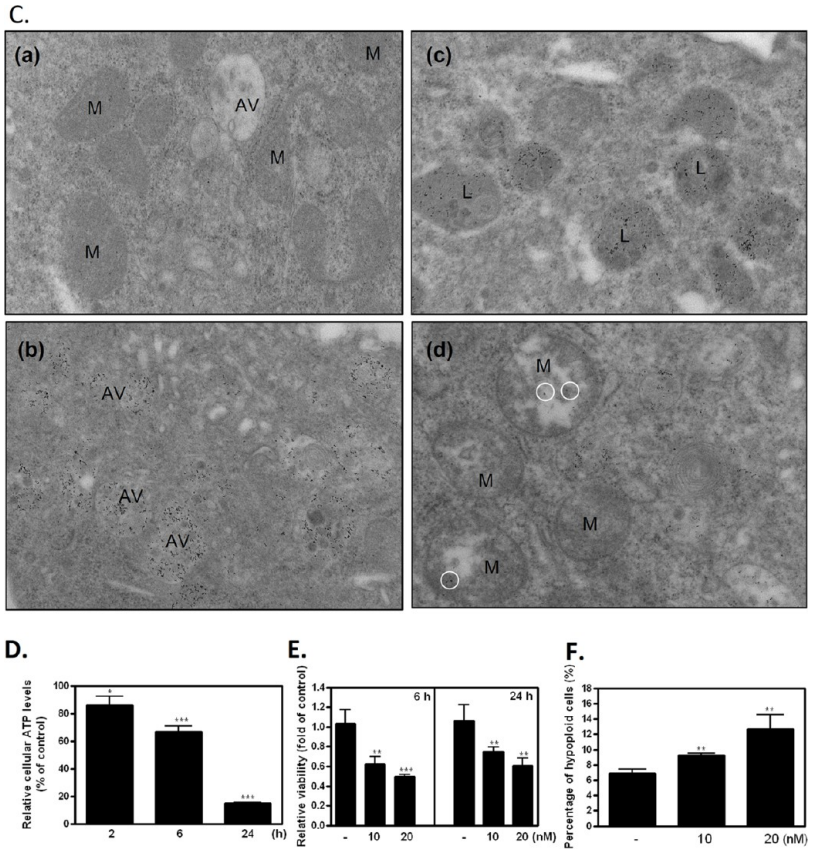

Figure 1. Distribution and effect of QDs. The intracellular distributions of QD in cells at 6 h (A) and 24 h (B). RAG cells were treated with 20 nM QDs (red), which was followed by staining with anticalnexin antibodies (green), anti-EEA1 antibodies (green), lysotracker (green), and mitotracker (green); the cells were then examined using confocal microscopy (magnification 1200×). Arrows indicate the colocalizations with QDs. (C) RAG cell, 15,000×. (a) Control: the autophagic vacuoles (AV) had a clear matrix with some cytological debris. Note that the mitochondria (M) have consistent material density. No lysosome was observed. (b,c) RAG cell; 40 nM QDs and 24 h. A large number of autophagic vacuoles (AV) and lysosomes (L) were observed in the cells. Note that large aggregations of dense particles, presumably QDs, were found in these autophagic vacuoles (AV) and lysosome (L). (d) RAG cell; 40 nM QDs and 24 h. Several swollen mitochondria were noted. These mitochondria had a rounded appearance with watery matrices. Careful examination also revealed scattered dense particles (white circles), presumably QD particles, in these mitochondria. (D) The ATP levels in 20 nM QD-treated cells at 2, 6, and 24 h. Mean ± standard deviations (SD), $n = 3$. RAG cells were treated with 10 and 20 nM QDs at 6 and 24 h. Cytotoxicity was determined at 24 h by MTT assay (E) and by PI staining with flow cytometry (F). Mean ± standard deviations, $n = 4$ (MTT assay); $n = 3$ (PI staining). (**, $p < 0.01$; ***, $p < 0.001$, compared with the untreated control).

RESULTS

Intracellular Distributions and Effects of QDs on the ER and Mitochondria. We used RAG cells as our model system because the kidney is the site of cadmium bioaccumulation. First, we investigated the uptake and the subcellular distribution and localization of QD at 6 and 24 h. Our results showed that QDs entered cells and were distributed to the ER, endosome, and lysosome at 6 h (Figure 1A), and located within mitochondria, endosome, and lysosome at 24 h (Figure 1B). Mitochondria activity is required for the MitoTracker dye to localize and be retained in mitochondria; MitoTracker only localizes in active mitochondria. Not all mitochondria were stained with QDs, indicating that there may be still other target organelles of the QD distribution or that some mitochondria activities may be affected by QDs. The dense collections of fine particles observed by TEM, presumably QDs, were found in both autophagic vacuoles and lysosomes at 24 h, as compared to the control (Figure 1C). Careful examination also revealed scattered fine particles in many mitochondria (Figure 1C, white circle). These fine particles were not observed in the mitochondria of control cells. It is also important to note that moderate mitochondrial edema (fluid mitochondrial matrix) and disintegration of mitochondria matrix were also evident in QD response cells (Figure 1C).

We further examined whether QDs were able to induce ER stress or mitochondrial dysfunction. ER stress is usually detected by measuring alterations in *ATF4* and *CHOP* expression. We found that the expression levels of *ATF4* and *CHOP* were not increased by the QDs suggesting that no ER stress had occurred at 6 and 24 h (data not shown). Next, we measured the cellular ATP level of the cells to determine whether QDs affected mitochondrial function. The results showed that 20 nM QDs substantially decreased cellular ATP levels at 2, 6, and 24 h in a time-dependent manner (Figure 1D). Therefore, QDs would seem to only affect mitochondrial function rather than induce ER stress. Moreover, treatment of RAG cells with 10 or 20 nM QDs reduced cell viability to approximately 40% to 70% of the untreated controls at 6 and 24 h (Figure 1E). To clarify the mechanism by which cell viability was reduced, we quantified cellular LDH activity using a conditioned culture medium, which is an indicator for cell necrosis.[38] QDs failed to cause any increase in LDH activity in the conditioned culture medium, which suggests that QDs did not induce cell necrosis (data not shown). However, QD

dx.doi.org/10.1021/tx300455k | *Chem. Res. Toxicol.* 2013, 26, 662−673

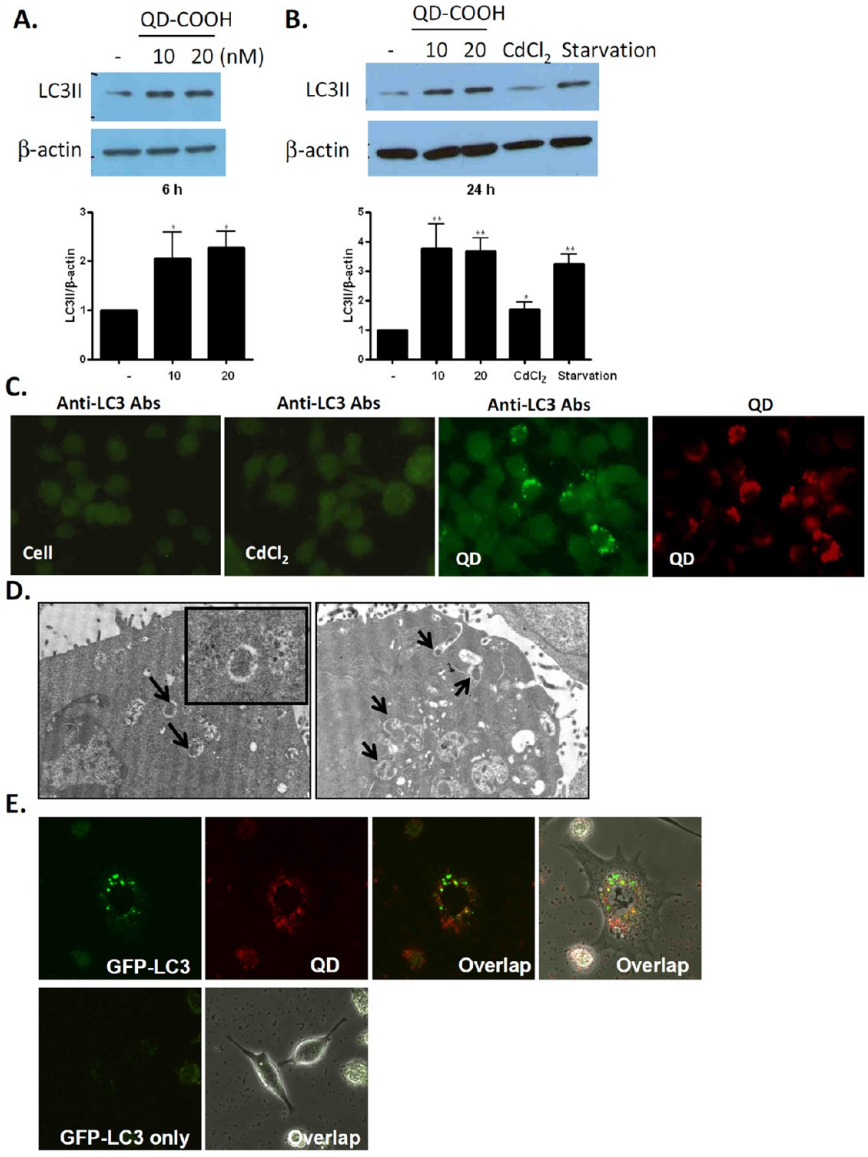

Figure 2. Autophagy in QD-treated cells. RAG cells were treated with 10 and 20 nM QD at 6 h (A) and 24 h (B). LC3 II and β-actin proteins were detected by immunoblotting and densitometry; the LC3 II/β-actin ratio is displayed. The densitometry ratio was analyzed by Image J in three independent experiments. Serum starvation of RAG cells was used as a positive result for autophagy (*, $p < 0.05$; **, $p < 0.01$, compared with the untreated control). (C) Immunofluorescence staining with LC3 antibody. RAG cells were treated for 24 h with control media (Cell), 21.66 μg/mL $CdCl_2$ (equivalent amount of Cd to 20 nM of QD as mentioned in the Materials and Methods), and 20 nM QD. QD fluorescence is displayed in red, and LC3 staining is displayed in green. Magnification 200×. (D) Electron microscopic images of RAG cells that were treated for 24 h with 20 nM QD. Black arrows show the autophagosome, which consist of double-layered membranes and contain cellular debris. Magnification 6000 and 15,000×. (E) RAG cells were transfected with GFP-LC3 for 5 h and then treated with 10 nM QD for another 18 h. The GFP-LC3 punctate formations were then examined using confocal microscopy (magnification 1200×).

treatment did increase the proportion of apoptotic cells, which were characterized using flow cytometry as having a hypoploid DNA fluorescence pattern (Figure 1F). The results from the TUNEL staining in RAG cells showed that QD treatment also induced cell apoptosis (Figure 4G). Taken together, these findings indicate that QDs were able to induce apoptosis in RAG cells.

Activation of Autophagy. Authophagy involves the breakdown of cellular components that can ensure cellular survival but is also suggested to be a form of cell death. LC3 is a ubiquitin-like protein, and it undergoes post-translational modifications whereby LC3 I becomes LC3 II. LC3 II insertion into the autophagosome membrane is a consistent key step in autophagosome formation, and its levels reflect the relative number of autophagosomes in the cells.[39] Treatment of RAG cells with 10 nM and 20 nM QDs caused the accumulation of LC3 II at 6 and 24 h (Figure 2A and B). Cadmium is the major toxic element in QDs. We used equal molarities of cadmium to clarify whether cadmium was able to induce autophagy. While QD treatment did cause clear LC3II accumulation in the cells, cadmium had only minor effects (Figure 2B and C). Although, released Cd ions might be responsible for the cytotoxicity of Cd-based QDs, other factors might also be involved in QD-induced cytotoxicity.[40] The ultrastructure of the RAG cells confirmed that QD treatment did cause the formation of the autophagosome in the cytoplasm (Figure 2D). The GFP-LC3 was visualized by confocal microscopy as punctate structures that represent autophagosomes (Figure 2E).

dx.doi.org/10.1021/tx300455k | Chem. Res. Toxicol. 2013, 26, 662−673

ROS Generation in QD-Treated Cells. It has been reported that NP-elicited ROS is associated with tissue injury and cell death. Although the generation of ROS is associated with QD-caused cytotoxicity, the role or function of ROS in the cytotoxicity of QDs remains unclear.[41] Taking the above into account, we found that treatment of RAG cells with QDs increased intracellular ROS levels at 2, 6, and 24 h (Figure 3A)

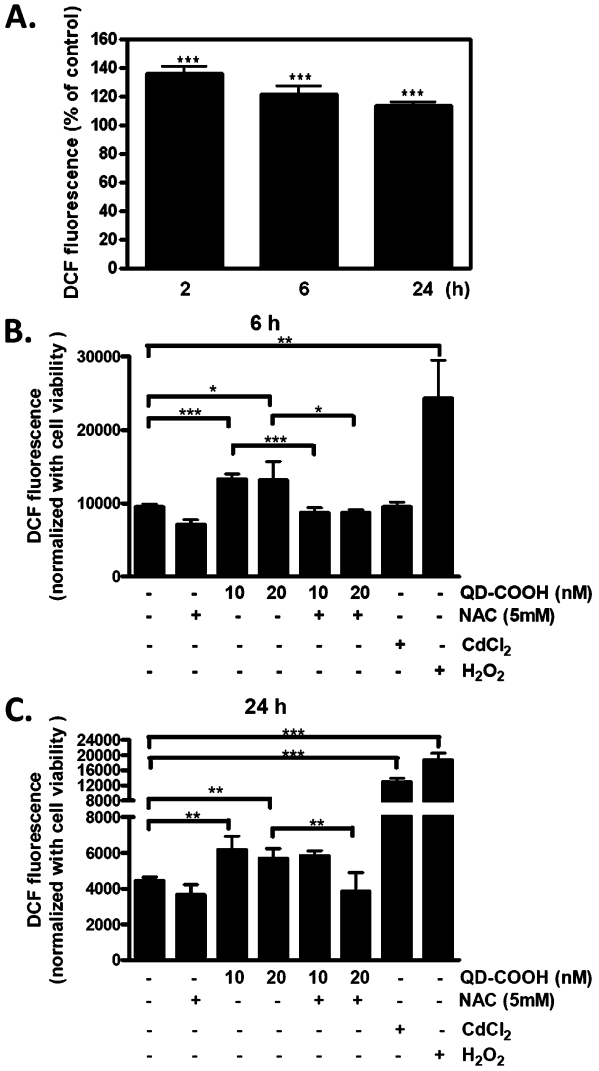

Figure 3. ROS generations in QD-treated cells. Intracellular ROS was detected by DCF fluorescence intensity measurement using a microplate reader. ROS production in RAG cells treated with 20 nM QDs at 2, 6, and 24 h (A). Mean ± standard deviations, $n = 4$. NAC (5 mM) pretreatment decreased QD-induced ROS production at 6 h (B) and 24 h (C). Cells treated with 10 μM H_2O_2 for 2 h were used as a positive control group. ROS levels were represented as DCF fluorescence, which was normalized with cell viability. Mean ± SD, $n = 8$ (***, $p < 0.001$, compared with the untreated control).

and that this was reduced by cotreatment with the antioxidant *N*-acetylcysteine (NAC) at 6 and 24 h (Figure 3B and C). Co-treatment with NAC did not change the intracellular uptake of QDs (data not shown). Cd failed to trigger ROS production until 24 h. However, our results showed that QDs can trigger autophagy formation at 6 and 24 h (Figure 2A).

Roles of ROS and Autophagy in the QD-Induced Cell Death. Mitochondrial dysfunction-elicited oxidative stress is able to cause the accumulation of cytotoxic mediators and cell death.[39] A number of studies have shown the essential role of ROS in the regulation of autophagic process.[42−44] A decrease in cellular mitochondrial membrane potential ($\Delta\Psi$) has been observed in response to many apoptotic stimuli.[45,46] However, it was also reported that ROS produced by damaged mitochondria seems to be able to induce mitophagy, which is the selective removal of mitochondria by autophagy; the function of this being the elimination of any damaged organelles. It was originally proposed that loss of $\Delta\Psi$ serves as a cue for mitophagy.[43] In order to examine the role of ROS in relation to QD-caused cytotoxicity, we cotreated RAG cells with NAC and QDs. The results showed that NAC reduced intracellular ROS levels but enhanced cell death after treatment with QD at 6 and 24 h (Figure 4A and B). In addition, NAC-enhanced cell death was found not to be related to necrosis at 6 or 24 h (Figure 4C and D). Furthermore, we used NAC to determine the effect of ROS on the mitochondrial $\Delta\Psi$ and the role of ROS in cell death in QD-treated cells. We found that NAC reduced mitochondrial $\Delta\Psi$ (Figure. 4E) and increased the number of hypoploid apoptotic cells (Figure 4F) as well as increasing the amount of apoptotic cells (Figure 4G). ROS has been found to be essential for autophagy induction and to specifically regulate the activity of autophagy-related protein 4.[42] Moreover, we found that NAC decreased QD-induced autophagy at 6 and 24 h (Figure 5). Our results indicated that the elevated levels of intracellular ROS positively regulated QD-induced autophagy. However, 3-MA, a PI3-kinase inhibitor, is one of the commonly used pharmacological approaches to the inhibition of autophagy *in vitro*.[47] We found that 3-MA reduced cell viability after QD treatment for 6 and 24 h (Figure 6). Therefore, we believed that oxidative stress-induced autophagy is a defense/survival mechanism against the cytotoxicity of QDs.

DISCUSSION

Previous studies have reported that NPs induced autophagy via a size-dependent mechanism.[20] It has been documented that smaller NPs have higher permeability and that this results in organelle dysfunction. Autophagy activation leads to exocytosis or destruction of the small NPs or to cell death.[20] Furthermore, it was reported that alpha-alumina NPs can induce efficient autophagy-dependent cross-presentation and potent antitumor response.[48] C60 NP can enhance the cytotoxicity of chemotherapeutic agents and reduce drug resistance by modulating autophagy, which may ultimately lead to novel therapeutic strategies in cancer therapy.[49] It is important to figure out the mechanisms and functions of autophagy induced by NPs. However, the function and mechanism of autophagy induced by NPs is still unknown. In our present study, we investigated the role and mechanism of QD in the induction of autophagy in RAG cells (Figure 7). QDs increased intracellular ROS levels and autophagy leading to cell death in RAG cells. Moreover, NAC reduced intracellular ROS levels, decreased QD-induced autophagy, but enhanced QD-induced cell death. We also use an autophagy inhibitor, 3MA, to determine the role of autophagy in QD-induced cell death. 3-MA at high concentrations (10 mM) not only targeted Class III PI3-kinase to inhibit initiation of autophagy but also disturbed the late stages of autophagy, such as lysosomal acidification.[47,50,51] Thus, 3-MA enhanced cell death in QD-treated cells. Taken together, it is clear that the inhibition of autophagy by 3-MA and NAC increased cell death, which supports the hypothesis

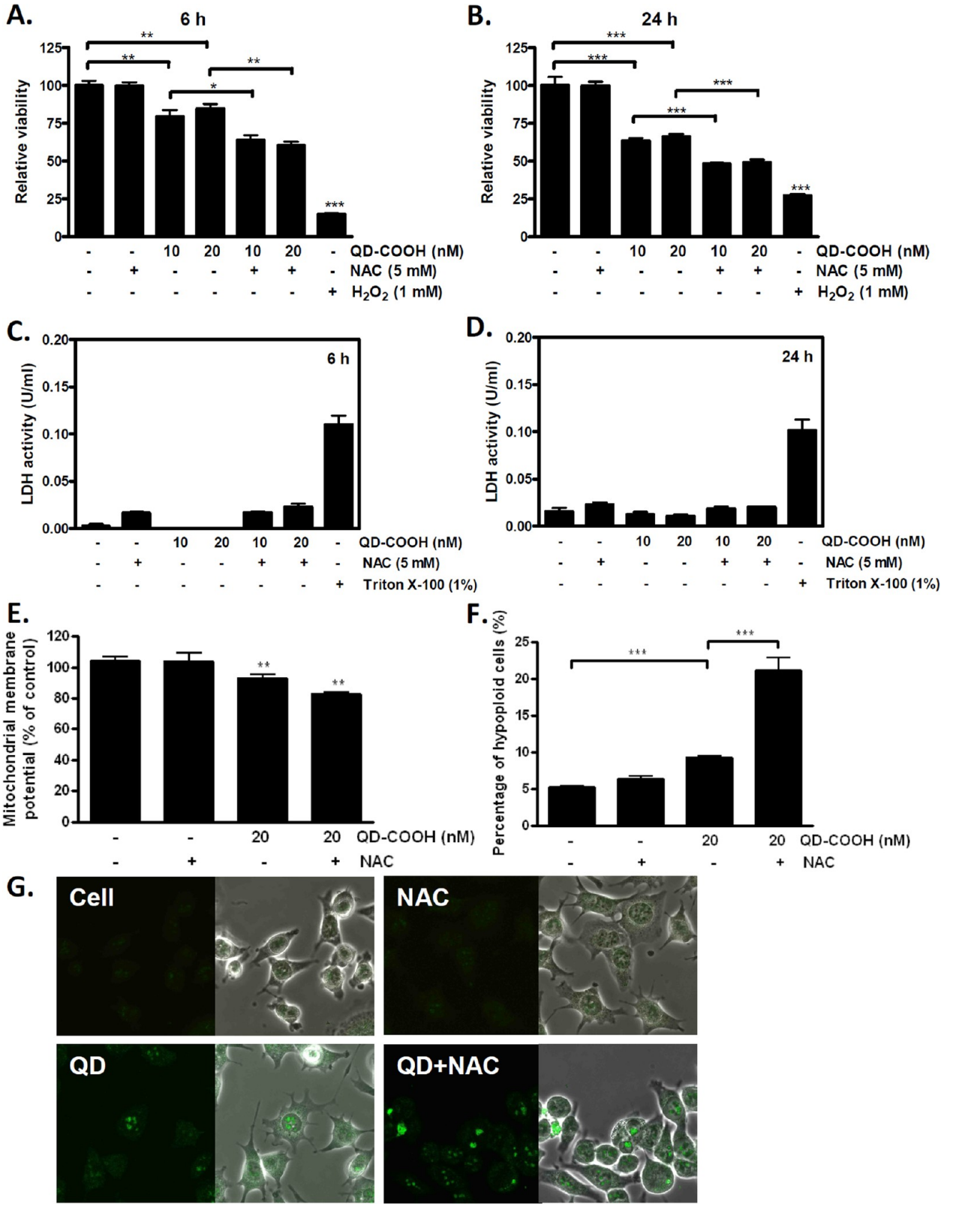

Figure 4. Effect of NAC on QD-induced adverse responses. Cytotoxicity was determined at each time point by the MTT assay (A and B) and LDH assay (C and D). Mean ± SD, $n = 4$ (*, $p < 0.05$; **, $p < 0.01$; ***, $p < 0.001$, compared with the untreated control). H_2O_2 (1 mM) treatment for 0.5 h was a positive control for the MTT assay. Treatment with 1% of triton X-100 was used as the positive control group for the LDH assay. The mitochondrial membrane potential $\Delta\Psi$ of the 20 nM QD-treated cells (E) and hypoploid apoptotic cell numbers (F) when treated with 20 nM QDs, both with or without NAC (5 mM) pretreatment. Mean ± SD, $n = 3$. (**, $p < 0.01$; ***, $p < 0.001$, compared with the untreated control). (G) RAG cells were treated with 20 nM QDs with or without NAC pretreatment. The TUNEL positive cells were detected by confocal microscopy (magnification 1200×).

dx.doi.org/10.1021/tx300455k | *Chem. Res. Toxicol.* 2013, 26, 662−673

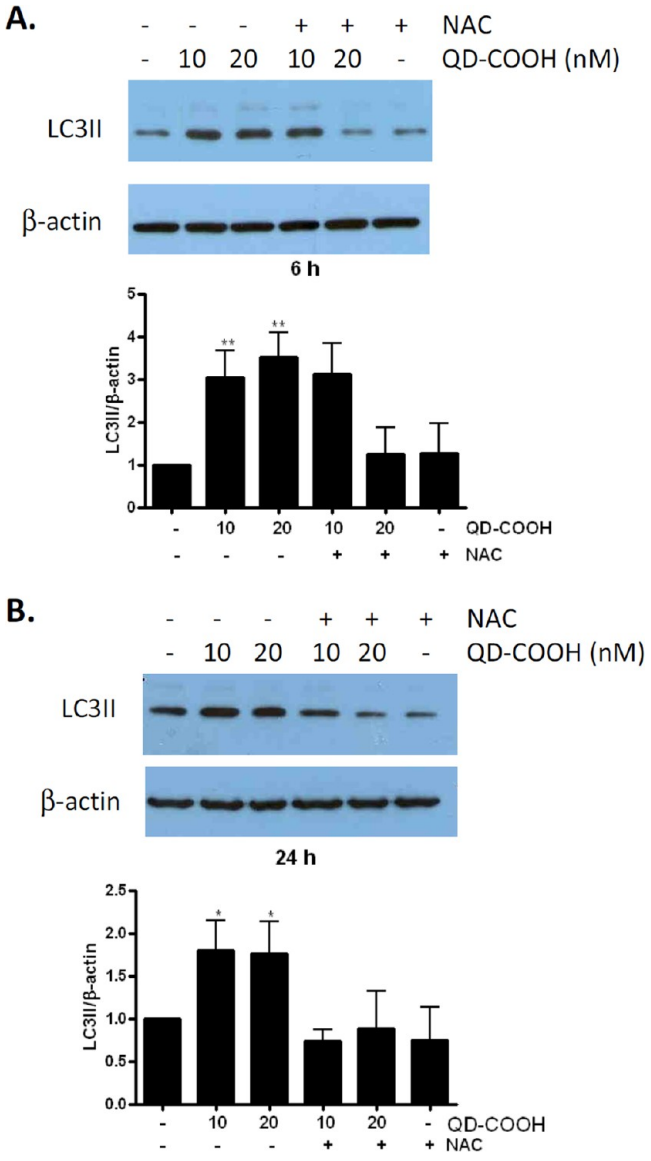

Figure 5. Effect of NAC on QD-induced autophagy. LC3 II expression in 10 and 20 nM QD-treated cells at 6 h (A) and 24 h (B) with or without NAC (5 mM) pretreatment. LC3 II and β-actin proteins were detected by immunoblotting; densitometry of the LC3 II/β-actin ratio is displayed. The densitometry ratio was analyzed by Image J in three repetitive experiments (*, $p < 0.05$; **, $p < 0.01$, compared with the untreated control).

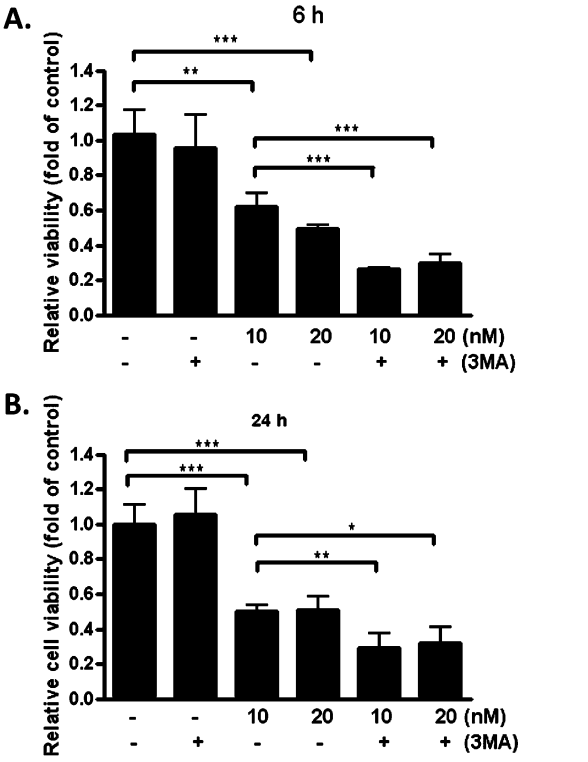

Figure 6. Effect of 3-MA on QD-induced cytotoxicity. 3-MA (10 mM) enhanced QD-induced cytotoxicity at 6 h (A) and 24 h (B). Cytotoxicity was determined by the MTT assay. Mean ± SD, $n = 4$ (*, $p < 0.05$; **, $p < 0.01$; ***, $p < 0.001$, compared with the untreated control).

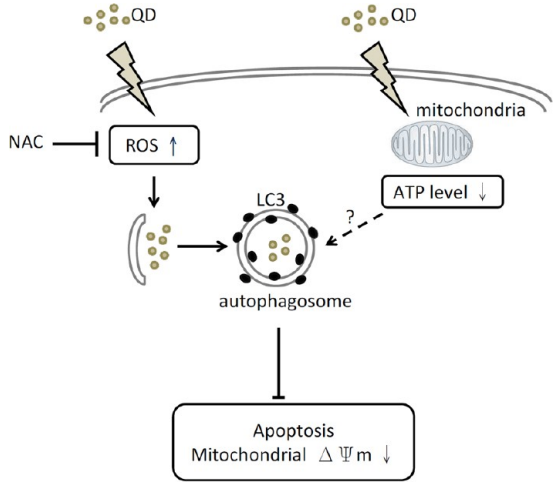

Figure 7. Model of oxidative stress and autophagy induced by QDs in RAG cells. NAC reduces intracellular ROS levels, decreases QD-induced autophagy, but enhances QD-induced cell death. ROS play an essential role in the regulation of QD-induced autophagy, which subsequently enhances cell survival. $\Delta\Psi$, mitochondrial membrane potential.

that autophagy is a cellular protective mechanism response to QD treatment.

Generation of ROS is believed to be the basis for QD-induced toxicity.[16,17,52,53] It has been proposed that the biological responses to oxidative stress induced by nanomaterials may occur in a three-tiered sequence.[41] Tier 1 of the sequence is the initial response to the challenge via cellular antioxidation defense. Tier 2 is the failure of the defense system due to overwhelming ROS accumulation, which is accompanied by the induction of oxidative stress and inflammation. Tier 3 is cytotoxicity due to mitochondrial damage, cellular injury, and apoptosis.[32] The results in the present study fit this three-tiered model. It was believed that the cytotoxicity of QDs is associated with the generation of ROS. Our result indicated that an appropriate amount of ROS is not harmful but essential to induce autophagy for survival. The initial ROS response to QD challenge is an induction of autophagy to allow self-clearance. Autophagy can be classified as a Tier 1 defense mechanism in the above sequence, although its function is not antioxidative in nature. A large amount of ROS accumulation is likely to be accompanied by an induction of mitochondrial dysfunction and cell death. Some studies showed that inhibition of ROS

dx.doi.org/10.1021/tx300455k | Chem. Res. Toxicol. 2013, 26, 662−673

production can be protective against cell death or DNA damage induced by NPs.[54−57] Our results showed that pretreatment with NAC was found to reduce ROS levels and that this resulted in an inhibition of autophagy and increase of cell death. Therefore, it would seem that NAC or 3-MA is able to repress the Tier 1 defense system and that this triggers further cell death. On the basis of our results, we proposed that whether the role of oxidative stress is good or harmful for cells may be dependent on the amounts of ROS and time point. Oxidative stress may be essential for cell survival to trigger autophagy in the initial stage. As increasing amounts of QDs enter into cells, overwhelming oxidative stress may be harmful to cells.

However, the cross-talk between autophagy, redox signaling, and mitochondrial dysfunction is not well understood.[39] Oxidative stress is indivisibly linked to mitochondrial dysfunction since mitochondria are both the generators of and the targets for reactive species.[58] Mitochondrial dysfunction leads to changes in membrane potential, ROS production, and ATP production.[59] One possibility is that there is an accumulation of toxic proteins followed by a decrease in mitochondrial function, which then leads to further overwhelming oxidative stress whereby the autophagic process is disrupted.[60−62] The sources of elevated ROS production may be either mitochondria themselves or plasma membrane oxidases,[63] and the mitochondria also may be the target of ROS. We also found that QD-induced autophagy occurred at 6 h, although ROS was already increasing at 2 h. Autophagic activities are known to be sensitive to ROS levels, but it is still unclear which source(s) of ROS elicit the autophagic responses in QD-treated cells.

A QD enters cells, is distributed to the ER, endosome, and lysosome at 6 h and located within the mitochondria, endosome, and lysosome at 24 h. Mitochondria, lysosome, and Golgi complex are several destinations of the endocytosed QD in murine macrophage-like cells (J774A.1), hepatocellular carcinoma (QGY), and rat basophilic leukemia (RBL) cell lines.[64,65] The ER not only is responsible for cellular protein synthesis and folding but also has an important role in sensing cellular stress.[66] An accumulation of misfolded proteins can cause ER stress and activate the unfolded protein response, which induces the expression of chaperones and other proteins involved in the recovery process. Several studies have demonstrated that ER and mitochondria are able to respond to silver and gold NP induced-oxidative stress further leading to cell death.[67−69] It has been reported that gold nanorods are able to selectively accumulate in the mitochondria of cancer cells. This long-term retention of gold nanorods decreased mitochondrial membrane potential and increased cellular ROS levels, which increased the likelihood of cell death.[70] However, our results showed that treatment with QDs failed to induce ER stress-related gene expression and that, rather, QD induced mitochondrial dysfunction.

Recently, it was proposed that biopersistent nanomaterials can negatively influence autophagy and endolysosomal pathways.[71] The gold nanoparticles induce autophagosome accumulation leading to the interruption of the autophagic pathway, by accumulating in lysosomes, and the impairment of lysosome degradation capacity.[72] Exposure to toxic concentrations of QDs results in ROS formation, mitochondrial swelling and loss of cristae, autophagy formation, and disturbed lysosome function in PC12 cells.[73] Soenen et al.[7] reported that QDs were found to localize in endosomes, where QDs generated ROS. QDs might be degraded in endosomes and leach free Cd ions. In the present study, we found that QDs distributed to the endosome, mitochondria, and lysosome at 24 h. The mitochondrial function and morphology were also affected by QDs. ROS triggered by QDs can positively regulate autophagy formation. In the future, we will explore how to evaluate the levels of QD in different intracellular organelles and whether QDs are exocytosed or interrupt lysosome functions in our model.

Several studies have developed QD-based therapeutics and used NPs for diagnostic purposes.[74−77] The development of multifunctional QDs that are visible, targetable, and capable of carrying a therapeutic payloads into cancer cells will continue to expand in the near future.[1,2,74] Therefore, it is important to understand the cellular defense mechanisms that are provoked by QDs. It was generally believed that oxidative stress is the toxic species that damages cellular organelles. It also has been suggested that autophagy is bad for cells because cells with multiple vesicles seem to be unhealthy. Excessive or abnormal free radical accumulation occurs in many diseases. Autophagy plays an important role in sensing oxidative stress, removing damaged proteins, removing damaged organelles, and eliminating the damaged cellular machinery that is responsible for excessive ROS production.[39] In agreement with the above, our results show that autophagy or "self-eating" can be good for cells and protect them from the ROS that is produced when QDs are internalized into cells. In summary, our results suggest that oxidative stress-induced autophagy is a defense/survival mechanism against the cytotoxicity of QDs.

■ ASSOCIATED CONTENT

Ⓢ Supporting Information

Shape and size of nanoparticles characterized by DLS and TEM. This material is available free of charge via the Internet at http://pubs.acs.org.

■ AUTHOR INFORMATION

Corresponding Author

*Tel: +886-37-246-266 ext. 36508. Fax: 886-37-587-406. E-mail: pplin@nhri.org.tw.

Funding

This work was supported by grant NM-099-PP08 and NM-100-PP08 from the Center for Nanomedicine Research, National Health Research Institutes, Zhunan, Taiwan.

Notes

The authors declare no competing financial interest.

■ ACKNOWLEDGMENTS

We acknowledge Dr. Ying-Jan Wang (Department of Environmental and Occupational Health, National Cheng Kung University, Medical College, Tainan, Taiwan) and Dr. Louis W. Chang (visiting scholar of National Environmental Health Research Center, National Health Research Institutes, Zhunan, Taiwan) for suggestions related to the TEM results.

■ ABBREVIATIONS

QDs, quantum dots; NAC, *N*-acetylcysteine; LDH, lactate dehydrogenase; DCF-DA, 2,7-dichlorofluorescein diacetate; $\Delta\Psi m$, mitochondrial membrane potential

REFERENCES

(1) Wang, Y., and Chen, L. (2011) Quantum dots, lighting up the research and development of nanomedicine. *Nanomedicine 7*, 385−402.

(2) Santra, S. (2012) The potential clinical impact of quantum dots. *Nanomedicine (London, U.K.) 7*, 623−626.

(3) Qi, L., and Gao, X. (2008) Emerging application of quantum dots for drug delivery and therapy. *Expert Opin. Drug Delivery 5*, 263−267.

(4) de la Zerda, A., and Gambhir, S. S. (2007) Drug delivery: keeping tabs on nanocarriers. *Nature Nanotechnol. 2*, 745−746.

(5) Michalet, X., Pinaud, F. F., Bentolila, L. A., Tsay, J. M., Doose, S., Li, J. J., Sundaresan, G., Wu, A. M., Gambhir, S. S., and Weiss, S. (2005) Quantum dots for live cells, in vivo imaging, and diagnostics. *Science 307*, 538−544.

(6) Hutter, E., and Maysinger, D. (2011) Gold nanoparticles and quantum dots for bioimaging. *Microsc. Res. Tech. 74*, 592−604.

(7) Soenen, S. J., Demeester, J., De Smedt, S. C., and Braeckmans, K. (2012) The cytotoxic effects of polymer-coated quantum dots and restrictions for live cell applications. *Biomaterials 33*, 4882−4888.

(8) Gao, X., Cui, Y., Levenson, R. M., Chung, L. W., and Nie, S. (2004) In vivo cancer targeting and imaging with semiconductor quantum dots. *Nature Biotechnol. 22*, 969−976.

(9) Wu, X., Liu, H., Liu, J., Haley, K. N., Treadway, J. A., Larson, J. P., Ge, N., Peale, F., and Bruchez, M. P. (2003) Immunofluorescent labeling of cancer marker Her2 and other cellular targets with semiconductor quantum dots. *Nature Biotechnol. 21*, 41−46.

(10) Hardman, R. (2006) A toxicologic review of quantum dots: toxicity depends on physicochemical and environmental factors. *Environ. Health Perspect. 114*, 165−172.

(11) Clift, M. J., Varet, J., Hankin, S. M., Brownlee, B., Davidson, A. M., Brandenberger, C., Rothen-Rutishauser, B., Brown, D. M., and Stone, V. (2011) Quantum dot cytotoxicity in vitro: an investigation into the cytotoxic effects of a series of different surface chemistries and their core/shell materials. *Nanotoxicology 5*, 664−674.

(12) Yildiz, I., Deniz, E., McCaughan, B., Cruickshank, S. F., Callan, J. F., and Raymo, F. M. (2010) Hydrophilic CdSe-ZnS core-shell quantum dots with reactive functional groups on their surface. *Langmuir 26*, 11503−11511.

(13) Yildiz, I., McCaughan, B., Cruickshank, S. F., Callan, J. F., and Raymo, F. M. (2009) Biocompatible CdSe-ZnS core-shell quantum dots coated with hydrophilic polythiols. *Langmuir 25*, 7090−7096.

(14) Aldana, J., Lavelle, N., Wang, Y., and Peng, X. (2005) Size-dependent dissociation pH of thiolate ligands from cadmium chalcogenide nanocrystals. *J. Am. Chem. Soc. 127*, 2496−2504.

(15) Dorvee, J. R., Derfus, A. M., Bhatia, S. N., and Sailor, M. J. (2004) Manipulation of liquid droplets using amphiphilic, magnetic one-dimensional photonic crystal chaperones. *Nat. Mater. 3*, 896−899.

(16) Lovric, J., Cho, S. J., Winnik, F. M., and Maysinger, D. (2005) Unmodified cadmium telluride quantum dots induce reactive oxygen species formation leading to multiple organelle damage and cell death. *Chem. Biol. 12*, 1227−1234.

(17) Ipe, B. I., Lehnig, M., and Niemeyer, C. M. (2005) On the generation of free radical species from quantum dots. *Small 1*, 706−709.

(18) Valko, M., Morris, H., and Cronin, M. T. (2005) Metals, toxicity and oxidative stress. *Current medicinal chemistry 12*, 1161−1208.

(19) Hauck, T. S., Anderson, R. E., Fischer, H. C., Newbigging, S., and Chan, W. C. W. (2010) In vivo quantum-dot toxicity assessment. *Small 6*, 138−144.

(20) Zabirnyk, O., Yezhelyev, M., and Seleverstov, O. (2007) Nanoparticles as a novel class of autophagy activators. *Autophagy 3*, 278−281.

(21) Li, J. J., Hartono, D., Ong, C. N., Bay, B. H., and Yung, L. Y. (2010) Autophagy and oxidative stress associated with gold nanoparticles. *Biomaterials 31*, 5996−6003.

(22) Stern, S. T., Zolnik, B. S., McLeland, C. B., Clogston, J., Zheng, J., and McNeil, S. E. (2008) Induction of autophagy in porcine kidney cells by quantum dots: a common cellular response to nanomaterials? *Toxicol. Sci. 106*, 140−152.

(23) Lee, C. M., Huang, S. T., Huang, S. H., Lin, H. W., Tsai, H. P., Wu, J. Y., Lin, C. M., and Chen, C. T. (2011) C60 fullerene-pentoxifylline dyad nanoparticles enhance autophagy to avoid cytotoxic effects caused by the beta-amyloid peptide. *Nanomedicine 7*, 107−114.

(24) Li, C., Liu, H., Sun, Y., Wang, H., Guo, F., Rao, S., Deng, J., Zhang, Y., Miao, Y., Guo, C., Meng, J., Chen, X., Li, L., Li, D., Xu, H., Li, B., and Jiang, C. (2009) PAMAM nanoparticles promote acute lung injury by inducing autophagic cell death through the Akt-TSC2-mTOR signaling pathway. *J. Mol. Cell Biol. 1*, 37−45.

(25) Rabinowitz, J. D., and White, E. (2010) Autophagy and metabolism. *Science 330*, 1344−1348.

(26) Moore, M. N. (2008) Autophagy as a second level protective process in conferring resistance to environmentally-induced oxidative stress. *Autophagy 4*, 254−256.

(27) Moore, M. N., Allen, J. I., and Somerfield, P. J. (2006) Autophagy: role in surviving environmental stress. *Mar. Environ. Res. 62* (Suppl), S420−S425.

(28) Cuervo, A. M. (2004) Autophagy: in sickness and in health. *Trends Cell Biol. 14*, 70−77.

(29) Mizushima, N., Levine, B., Cuervo, A. M., and Klionsky, D. J. (2008) Autophagy fights disease through cellular self-digestion. *Nature 451*, 1069−1075.

(30) Yang, R. S., Chang, L. W., Wu, J. P., Tsai, M. H., Wang, H. J., Kuo, Y. C., Yeh, T. K., Yang, C. S., and Lin, P. (2007) Persistent tissue kinetics and redistribution of nanoparticles, quantum dot 705, in mice: ICP-MS quantitative assessment. *Environ. Health Perspect. 115*, 1339−1343.

(31) Lin, C. H., Chang, L. W., Chang, H., Yang, M. H., Yang, C. S., Lai, W. H., Chang, W. H., and Lin, P. (2009) The chemical fate of the Cd/Se/Te-based quantum dot 705 in the biological system: toxicity implications. *Nanotechnology 20*, 215101.

(32) Lin, C. H., Yang, M. H., Chang, L. W., Yang, C. S., Chang, H., Chang, W. H., Tsai, M. H., Wang, C. J., and Lin, P. (2011) Cd/Se/Te-based quantum dot 705 modulated redox homeostasis with hepatotoxicity in mice. *Nanotoxicology 5*, 650−663.

(33) Yeh, T. K., Wu, J. P., Chang, L. W., Tsai, M. H., Chang, W. H., Tsai, H. T., Yang, C. S., and Lin, P. (2011) Comparative tissue distributions of cadmium chloride and cadmium-based quantum dot 705 in mice: Safety implications and applications. *Nanotoxicology 5*, 91−97.

(34) Alley, M. C., Scudiero, D. A., Monks, A., Hursey, M. L., Czerwinski, M. J., Fine, D. L., Abbott, B. J., Mayo, J. G., Shoemaker, R. H., and Boyd, M. R. (1988) Feasibility of drug screening with panels of human tumor cell lines using a microculture tetrazolium assay. *Cancer Res. 48*, 589−601.

(35) Do, T. N., Rosal, R. V., Drew, L., Raffo, A. J., Michl, J., Pincus, M. R., Friedman, F. K., Petrylak, D. P., Cassai, N., Szmulewicz, J., Sidhu, G., Fine, R. L., and Brandt-Rauf, P. W. (2003) Preferential induction of necrosis in human breast cancer cells by a p53 peptide derived from the MDM2 binding site. *Oncogene 22*, 1431−1444.

(36) Krysko, D. V., Vanden Berghe, T., D'Herde, K., and Vandenabeele, P. (2008) Apoptosis and necrosis: detection, discrimination and phagocytosis. *Methods 44*, 205−221.

(37) McGinnes, K., Chapman, G., and Penny, R. (1988) Effects of interferon on natural killer (NK) cells assessed by fluorescent probes and flow cytometry. *J. Immunol. Methods 107*, 129−136.

(38) Cai, L., Wang, H., Li, Q., Qian, Y., and Yao, W. (2008) Salidroside inhibits H2O2-induced apoptosis in PC12 cells by preventing cytochrome c release and inactivating of caspase cascade. *Acta Biochim. Biophys. Sin. 40*, 796−802.

(39) Lee, J., Giordano, S., and Zhang, J. (2012) Autophagy, mitochondria and oxidative stress: cross-talk and redox signalling. *Biochem. J. 441*, 523−540.

(40) Chen, N., He, Y., Su, Y., Li, X., Huang, Q., Wang, H., Zhang, X., Tai, R., and Fan, C. (2012) The cytotoxicity of cadmium-based quantum dots. *Biomaterials 33*, 1238−1244.

(41) Nel, A., Xia, T., Madler, L., and Li, N. (2006) Toxic potential of materials at the nanolevel. *Science 311*, 622−627.

(42) Scherz-Shouval, R., Shvets, E., Fass, E., Shorer, H., Gil, L., and Elazar, Z. (2007) Reactive oxygen species are essential for autophagy and specifically regulate the activity of Atg4. *EMBO J. 26*, 1749−1760.
(43) Scherz-Shouval, R., and Elazar, Z. (2011) Regulation of autophagy by ROS: physiology and pathology. *Trends Biochem. Sci. 36*, 30−38.
(44) Huang, J., Lam, G. Y., and Brumell, J. H. (2011) Autophagy signaling through reactive oxygen species. *Antioxid. Redox Signal. 14*, 2215−2231.
(45) Zamzami, N., Marchetti, P., Castedo, M., Decaudin, D., Macho, A., Hirsch, T., Susin, S. A., Petit, P. X., Mignotte, B., and Kroemer, G. (1995) Sequential reduction of mitochondrial transmembrane potential and generation of reactive oxygen species in early programmed cell death. *J. Exp. Med. 182*, 367−377.
(46) Gottlieb, E., Armour, S. M., Harris, M. H., and Thompson, C. B. (2003) Mitochondrial membrane potential regulates matrix configuration and cytochrome c release during apoptosis. *Cell Death Differ. 10*, 709−717.
(47) Mizushima, N., Yoshimori, T., and Levine, B. (2010) Methods in mammalian autophagy research. *Cell 140*, 313−326.
(48) Li, H. Y., Li, Y. H., Jiao, J., and Hu, H. M. (2011) Alpha-alumina nanoparticles induce efficient autophagy-dependent cross-presentation and potent antitumour response. *Nat. Nanotechnol. 6*, 645−650.
(49) Wei, P. F., Zhang, L., Lu, Y., Man, N., and Wen, L. P. (2010) C60(Nd) nanoparticles enhance chemotherapeutic susceptibility of cancer cells by modulation of autophag. *Nanotechnology*, 21.
(50) Caro, L. H., Plomp, P. J., Wolvetang, E. J., Kerkhof, C., and Meijer, A. J. (1988) 3-Methyladenine, an inhibitor of autophagy, has multiple effects on metabolism. *Eur. J. Biochem. 175*, 325−329.
(51) Mizushima, N., Yamamoto, A., Hatano, M., Kobayashi, Y., Kabeya, Y., Suzuki, K., Tokuhisa, T., Ohsumi, Y., and Yoshimori, T. (2001) Dissection of autophagosome formation using Apg5-deficient mouse embryonic stem cells. *J. Cell Biol. 152*, 657−668.
(52) Samia, A. C., Chen, X., and Burda, C. (2003) Semiconductor quantum dots for photodynamic therapy. *J. Am. Chem. Soc. 125*, 15736−15737.
(53) Cho, S. J., Maysinger, D., Jain, M., Roder, B., Hackbarth, S., and Winnik, F. M. (2007) Long-term exposure to CdTe quantum dots causes functional impairments in live cells. *Langmuir 23*, 1974−1980.
(54) Hanley, C., Thurber, A., Hanna, C., Punnoose, A., Zhang, J. H., and Wingett, D. G. (2009) The influences of cell type and ZnO nanoparticle size on immune cell cytotoxicity and cytokine induction. *Nanoscale Res. Lett. 4*, 1409−1420.
(55) Pan, Y., Leifert, A., Ruau, D., Neuss, S., Bornemann, J., Schmid, G., Brandau, W., Simon, U., and Jahnen-Dechent, W. (2009) Gold nanoparticles of diameter 1.4 nm trigger necrosis by oxidative stress and mitochondrial damag. *Small 5*, 2067−2076.
(56) Li, K. G., Chen, J. T., Bai, S. S., Wen, X., Song, S. Y., Yu, Q., Li, J., and Wang, Y. Q. (2009) Intracellular oxidative stress and cadmium ions release induce cytotoxicity of unmodified cadmium sulfide quantum dots. *Toxicol. in Vitro 23*, 1007−1013.
(57) Sharma, V., Anderson, D., and Dhawan, A. (2012) Zinc oxide nanoparticles induce oxidative DNA damage and ROS-triggered mitochondria mediated apoptosis in human liver cells (HepG2). *Apoptosis 17*, 852−870.
(58) Murphy, M. P. (2009) How mitochondria produce reactive oxygen species. *Biochem. J. 417*, 1−13.
(59) Yen, W. L., and Klionsky, D. J. (2008) How to live long and prosper: autophagy, mitochondria, and aging. *Physiology 23*, 248−262.
(60) Hashimoto, M., Rockenstein, E., Crews, L., and Masliah, E. (2003) Role of protein aggregation in mitochondrial dysfunction and neurodegeneration in Alzheimer's and Parkinson's diseases. *Neuromol. Med. 4*, 21−36.
(61) Gottlieb, R. A., and Carreira, R. S. (2010) Autophagy in health and disease. 5. Mitophagy as a way of life. *Am. J. Physiol. 299*, C203−C210.
(62) Schneider, L., and Zhang, J. (2010) Lysosomal function in macromolecular homeostasis and bioenergetics in Parkinson's disease. *Mol. Neurodegener. 5*, 14.
(63) Thannickal, V. J., and Fanburg, B. L. (2000) Reactive oxygen species in cell signaling. *Am. J. Physiol. 279*, L1005−L1028.
(64) Zhang, Y., Mi, L., Xiong, R. L., Wang, P. N., Chen, J. Y., Yang, W. L., Wang, C. C., and Peng, Q. (2009) Subcellular localization of thiol-capped CdTe quantum dots in living cells. *Nanoscale Res. Lett. 4*, 606−612.
(65) Clift, M. J. D., Brandenberger, C., Rothen-Rutishauser, B., Brown, D. M., and Stone, V. (2011) The uptake and intracellular fate of a series of different surface coated quantum dots in vitro. *Toxicology 286*, 58−68.
(66) Zhang, K., and Kaufman, R. J. (2008) From endoplasmic-reticulum stress to the inflammatory response. *Nature 454*, 455−462.
(67) Tsai, Y. Y., Huang, Y. H., Chao, Y. L., Hu, K. Y., Chin, L. T., Chou, S. H., Hour, A. L., Yao, Y. D., Tu, C. S., Liang, Y. J., Tsai, C. Y., Wu, H. Y., Tan, S. W., and Chen, H. M. (2011) Identification of the nanogold particle-induced endoplasmic reticulum stress by omic techniques and systems biology analysis. *ACS Nano 5*, 9354−9369.
(68) Zhang, R., Piao, M. J., Kim, K. C., Kim, A. D., Choi, J.-Y., Choi, J., and Hyun, J. W. (2012) Endoplasmic reticulum stress signaling is involved in silver nanoparticles-induced apoptosis. *Int. J. Biochem. Cell Biol. 44*, 9.
(69) Bouwmeester, H., Poortman, J., Peters, R. J., Wijma, E., Kramer, E., Makama, S., Puspitaninganindita, K., Marvin, H. J., Peijnenburg, A. A., and Hendriksen, P. J. (2011) Characterization of translocation of silver nanoparticles and effects on whole-genome gene expression using an in vitro intestinal epithelium coculture model. *ACS Nano 5*, 4091−4103.
(70) Wang, L., Liu, Y., Li, W., Jiang, X., Ji, Y., Wu, X., Xu, L., Qiu, Y., Zhao, K., Wei, T., Li, Y., Zhao, Y., and Chen, C. (2011) Selective targeting of gold nanorods at the mitochondria of cancer cells: implications for cancer therapy. *Nano Lett. 11*, 772−780.
(71) Stern, S. T., Adiseshaiah, P. P., and Crist, R. M. (2012) Autophagy and lysosomal dysfunction as emerging mechanisms of nanomaterial toxicity. *Part. Fibre Toxicol. 9*, 20.
(72) Ma, X., Wu, Y., Jin, S., Tian, Y., Zhang, X., Zhao, Y., Yu, L., and Liang, X. J. (2011) Gold nanoparticles induce autophagosome accumulation through size-dependent nanoparticle uptake and lysosome impairment. *ACS Nano 5*, 8629−8639.
(73) Neibert, K. D., and Maysinger, D. (2012) Mechanisms of cellular adaptation to quantum dots–the role of glutathione and transcription factor EB. *Nanotoxicology 6*, 249−262.
(74) Jokerst, J. V., and Gambhir, S. S. (2011) Molecular imaging with theranostic nanoparticles. *Acc. Chem. Res. 44*, 1050−1060.
(75) Zhang, H., Yee, D., and Wang, C. (2008) Quantum dots for cancer diagnosis and therapy: biological and clinical perspectives. *Nanomedicine (London, U.K.) 3*, 83−91.
(76) Jain, K. K. (2007) Applications of nanobiotechnology in clinical diagnostics. *Clin. Chem. 53*, 2002−2009.
(77) Sahoo, S. K., Parveen, S., and Panda, J. J. (2007) The present and future of nanotechnology in human health care. *Nanomedicine 3*, 20−31.